Slowing of Magnetic Reconnection Concurrent with Weakening Plasma Inflows and Increasing Collisionality in Strongly Driven Laser-Plasma Experiments

M. J. Rosenberg, C. K. Li, W. Fox, A. B. Zylstra, C. Stoeckl, F. H. Séguin, J. A. Frenje, and R. D. Petrasso

Phys. Rev. Lett. **114**, 205004 — Published 20 May 2015

DOI: 10.1103/PhysRevLett.114.205004

Slowing of Magnetic Reconnection Concurrent with Weakening Plasma Inflows and Increasing Collisionality in Strongly-Driven Laser-Plasma Experiments

M. J. Rosenberg,[1,*] C. K. Li,[1] W. Fox,[2] A. B. Zylstra,[1] C. Stoeckl,[3] F. H. Séguin,[1] J. A. Frenje,[1] and R. D. Petrasso[1]

[1] *Plasma Science and Fusion Center, Massachusetts Institute of Technology, Cambridge, MA 02139, USA*
[2] *Princeton Plasma Physics Laboratory, Princeton, NJ 08543, USA*
[3] *Laboratory for Laser Energetics, University of Rochester, Rochester, NY 14623, USA*

(Dated: April 9, 2015)

An evolution of magnetic reconnection behavior, from fast jets to the slowing of reconnection and the establishment of a stable current sheet, has been observed in strongly-driven, $\beta \lesssim 20$ laser-produced plasma experiments. This process has been inferred to occur alongside a slowing of plasma inflows carrying the oppositely-directed magnetic fields as well as the evolution of plasma conditions from collisionless to collisional. High-resolution proton radiography has revealed unprecedented detail of the forced interaction of magnetic fields and super-Alfvénic electron jets ($V_{jet} \sim 20 V_A$) ejected from the reconnection region, indicating that two-fluid or collisionless magnetic reconnection occurs early in time. The absence of jets and the persistence of strong, stable magnetic fields at late times indicates that the reconnection process slows down, while plasma flows stagate and plasma conditions evolve to a cooler, denser, more collisional state. These results demonstrate that powerful initial plasma flows are not sufficient to force a complete reconnection of magnetic fields, even in the strongly-driven regime.

PACS numbers: 52.35.Vd, 52.50.Jm

Magnetic reconnection [1] is a ubiquitous phenomenon in space [2, 3] and laboratory [4] plasmas, where oppositely-directed magnetic fields undergo a modification of field-line topology and release magnetic energy. While reconnection has typically been studied experimentally in tenuous, quasi-steady-state plasmas, reconnection of magnetic fields in strongly-driven (ram pressure>magnetic pressure), β>1 (total thermal pressure>magnetic pressure) plasmas occurs frequently in astrophysics, impacting dynamics of plasmas in the solar photosphere [5] and at the heliopause [6]. In these strongly-driven environments, the rate of reconnection is dictated largely by hydrodynamics and the plasma flows that advect the magnetic fields.

In addition, when the scale width of the reconnection region is smaller than the ion inertial length ($d_i \equiv c/\omega_{pi}$), electrons and ions decouple, and the reconnection process is governed by electron flows, rather than by the entire plasma fluid. This two-fluid reconnection (otherwise known as Hall reconnection or collisionless reconnection) is faster than classical Sweet-Parker [7, 8] reconnection in the collisional, single-fluid regime. Two-fluid reconnection is a common occurrence in astrophysics [9] and it has been studied in tenuous, quasi-steady plasma experiments [10, 11]. Two-fluid reconnection in the high β or strongly-driven regimes is especially pertinent at the dayside magnetopause of the Earth and other planets [12, 13], though to date, there has been little laboratory investigation of the physics of two-fluid reconnection in such plasmas.

This Letter presents the direct observation of two-fluid reconnection features – fast electron jets – preceding the stagnation of magnetic fields and the establishment of a stable current sheet in a strongly-driven, $\beta \lesssim 20$ plasma experiment. These experiments were conducted using laser-produced plasmas, a well-established platform for studies of high-β magnetic reconnection. Prior experiments have examined the annihilation of magnetic fields [14–17], thermal properties of the plasma [18, 19], plasma jets [18, 20–22], and energetic electrons produced during reconnection [23]. Particle-in-cell simulations have predicted that, in addition to flux pileup, two-fluid physics plays a significant role in these strongly-driven, quasi-collisionless reconnection configurations [24]. In the present experiments, high-resolution proton radiography has produced images of unprecedented detail and clarity of colliding laser-produced plasmas where the reconnection of magnetic fields is occurring, revealing a striking evolution of reconnection behavior. The electron jets, a signature of two-fluid reconnection, emerge early in time when the plasma is forcefully driven and in a collisionless regime. Later in the collision process, the jet structures disappear and strong magnetic fields persist around the reconnection region, indicating a stalled reconnection. Based on plasma properties inferred from a combination of experimental data and hydrodynamic simulations, during this time the strong inflows weaken and the plasma also becomes more collisional. These results demonstrate that the magnetic fields may be stabilized by the slowing of the flows that strongly drive reconnection and also by the evolution of plasma conditions from collisionless to collisional.

Reconnection experiments using laser-produced plasmas were conducted at the OMEGA-EP laser facility [25]. In each experiment, depicted in Figure 1, a 12-μm-thick CH foil (1:1 atomic proportion at a density of 1.11

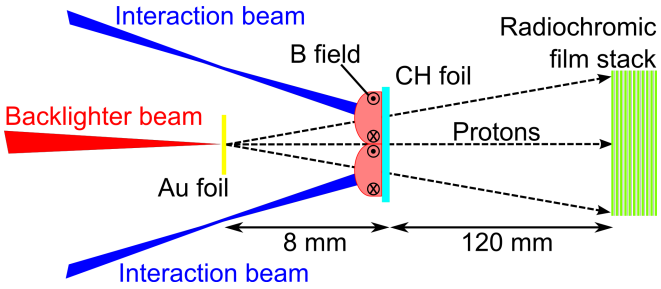

FIG. 1. (Color online) Proton radiography setup for reconnection experiments on OMEGA-EP.

g/cm^3) was irradiated by two 930-J, 1-ns laser pulses at a wavelength of 351 nm and with an 800-μm spot size. The laser spots were separated on the foil by 1.4 mm, each producing an expanding, hemispherical plasma bubble with an azimuthal magnetic field concentrated at its perimeter [26]. These plasmas expanded into each other, forcing their oppositely-directed magnetic fields to interact and reconnect.

The reconnecting plasma bubbles were imaged using proton radiography. The deflection of protons was used to infer local magnetic field structures and the spatial scale of field-carrying features in the plasma [27, 28]. Protons at energies up to ~60 MeV in an exponentially decaying spectrum were generated by a high-intensity (190-J, 1-ps duration, 10-20 μm spot size, ~10^{19} W/cm^2) laser incident on a 10-μm-thick Au foil, via the target normal sheath acceleration mechanism [29–31]. This backlighter foil was positioned 8 mm from the CH target foil and parallel to it. Backlighter protons were detected by a stack of radiochromic film (RCF) [32], with the pieces of film sensitive to protons at a variety of incident energies.

Proton radiographs obtained with ~18-MeV and ~24-MeV protons are shown in Figure 2. These radiographs were obtained in separate experiments at different times relative to the onset of the interaction beams. The fluence modulations across the images are largely due to the deflection of backlighter protons by magnetic fields around the laser-produced plasma bubbles and in their interaction.

The images reveal several signatures of magnetic fields and the dynamics of reconnection. The most readily apparent feature is the concentration of protons in a circular pattern around each bubble due to their inward deflection by ~MG azimuthal magnetic fields at the bubble perimeters. For laser and backlighter proton propagation into the page, these magnetic fields are oriented clockwise. These fields are generated by the Biermann battery mechanism [33], arising due to non-parallel gradients in electron density (into the page) and electron temperature (radially inward toward the center of each plasma bubble), with $\partial \mathbf{B}/\partial t \propto \nabla T_e \times \nabla n_e$.

A prevalent signature of fast, two-fluid reconnection, electron jets appear to be ejected out of the reconnection region along the current sheet early in time (Figure 2b). Based on their appearance at t=0.9 ns, extending out of the field of view, these structures have propagated continuously at least 800 μm over a period of ~600 ps, at an in-plane velocity of V_{jet}>1300 μm/ns. This velocity is considerably faster than the nominal ion Alfvén speed (V_{jet}~$20V_{A0}$), of the order of the electron Alfvén speed (V_{jet}~$0.3V_{Ae0}$), and several times the sound speed (V_{jet}~$5C_s$). The features are well-collimated, with a total apparent width of 150 μm ~$5d_i$, of order the expected width of the current sheet. They appear to consist of multiple near-parallel strands, each of which is of order ~d_i in width, extending at least 25 d_i from the end of the collision region. Based on the speed, length, and width of these features, which are similar to reconnection-related electron jets observed in two-fluid simulations [34], spacecraft observations of the magnetosheath [35], and similar laser-plasma experiments [22], the structures are interpreted as reconnection-induced electron jets. These jets arise self-consistently with in-plane currents typically ascribed to Hall or two-fluid reconnection physics. Notably, jets are not visible at later times, suggesting a stalled reconnection.

The deficit of protons in the collision region provides information about the large-scale magnetic fields in the reconnection region and further evidence of a slowing of the reconnection process at late times. These fields deflect protons out of the current sheet towards the center of each individual bubble. A lower bound on the magnetic field strength around the reconnection layer is inferred from width of the proton fluence deficit Δz in the interaction region (as shown in Figure 2b). At t=0.9 ns, Δz is ~280 μm at the foil in the 24-MeV-proton image, and is found to be ~280 μm as well in the image produced by 36-MeV protons, the highest energy for which a usable image was obtained. The highest proton energy is used to establish the largest possible lower bound on the path-integrated magnetic field magnitude. The path-integrated field strength in the proton deficit region is inferred on the basis that protons directed through the center of the current sheet were deflected at least a distance $\Delta z/2$ to the boundary of the proton deficit region. Quantitatively, this lower limit is inferred as

$$|\int \mathbf{B} \times \mathbf{dl}| > \frac{m_p v_p}{q} \frac{D}{a(D-a)} |\boldsymbol{\xi}|, \qquad (1)$$

where v_p is the velocity of protons at 36 MeV, the most likely proton energy on that film, D (a) is the backlighter-film (backlighter-foil) distance, and ξ=$\Delta z/2$ is the apparent proton deflection at the foil, the 140 μm half-width of the proton deficit region. For these conditions at t = 0.9 ns, $|\int \mathbf{B}\times\mathbf{dl}|$ >160 MG μm on either side of the current sheet. For a characteristic out-of-plane height for the magnetic field structure of dl ~300 μm, a reasonable

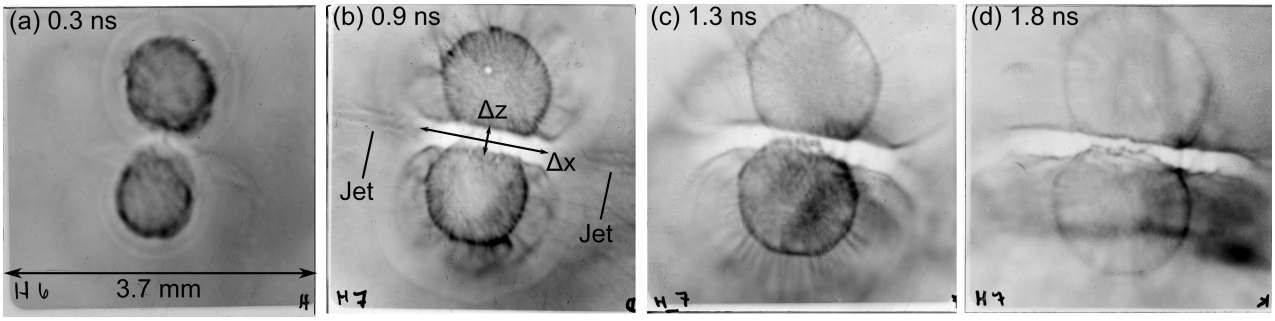

FIG. 2. Proton radiography images at different times relative to the onset of the interaction beams, with dark areas representing greater proton fluence. The image at (a) 0.3 ns is produced by ∼18-MeV protons, while the images at (b) 0.9 ns, (c) 1.3 ns, and (d) 1.8 ns are produced by ∼24-MeV protons. Contrast has been optimized differently in each image to reveal details. The times indicated are between the onset of the interaction beams and the arrival of backlighter protons.

assumption for early times in this class of experiment [33] and consistent with the plasma scale height in 2D DRACO [36] radiation-hydrodynamics simulations (discussed in more detail below), a magnetic field strength of $B \gtrsim 0.55$ MG is inferred. Based on prior experiments on OMEGA at half the laser energy as in the present OMEGA-EP experiments, in which a magnetic field strength of $B \sim 0.5$ MG was inferred [16, 33], the average magnetic field strength in the present experiments is likely no more than a factor of 2 greater than the lower-bound estimate. The length and width of the proton fluence feature and resulting estimates of magnetic-field quantities in the reconnection region at different times are summarized in Table I.

The images in Figure 2 show that the overall smoothness and width of the proton deflection pattern around the reconnection region does not significantly change between 0.9 ns and 1.8 ns. The appearance of this feature is used here as a proxy for the rate of reconnection, which cannot be directly calculated due to the lower-bound nature of the magnetic field measurements. Its stability illustrates a lack of magnetic flux annihilation and persistence of a long-lived and stable current sheet. During this late-time period, the magnetic fields are simply squeezed into the elongating collision midplane.

The appearance of a stable, stationary current sheet, bearing qualitative resemblence to a Sweet-Parker current sheet in the collisional reconnection picture, is remarkably different than has been observed in similar experiments where the magnetic field structure has rapidly disrupted [17]. In the present experiments, the current sheet persists much longer than would be expected based on an annihilation of magnetic fields at the initial plasma flow velocity, which has been observed in previous experiments [16] – for a proton deficit region width of $\Delta z \sim 280$ μm and an initial plasma flow velocity of $V \sim 700$ μm/ns, the time for the plasma to cross the reconnection region unimpeded is only ∼0.4 ns; however, the current sheet persists nearly unchanged for at least 0.9 ns. The persistence of the current sheet in the present experiments also necessarily implies that the current sheet is sufficiently thick so as to be stable to the tearing or plasmoid instability over the duration of the experiments. This can plausibly be explained by a calculation of the resistive tearing mode maximum growth rate [37], $\gamma_{max} \sim V_A/w(L/w)^{1/2}S^{-1/2}$, where V_A is the Alfvén speed, L is the current sheet width (taken as the measured Δx), w is the current sheet width (taken to be $\sim \Delta z/2$), and S is the Lundquist number, the ratio of diffusive to Alfvén timescales. For plasma conditions achieved in these experiments, γ_{max} is $\sim 1.1 \times 10^8$ s^{-1} (early times) or $\sim 7.1 \times 10^7$ s^{-1} (late times) . Over the ∼ns duration of the experiment, instability growth is minimal, no greater than ∼0.1. Notably, the formation of plasmoids was observed in simulations of similar experiments [38], but not in these experiments.

TABLE I. Estimates of magnetic-field quantities around the reconnection region at different times based on 36-MeV-proton images, including the full width of the proton fluence deficit region Δz, a lower bound on the inferred path-integrated field strength $|\int \mathbf{B} \times \mathbf{dl}|$, the approximate characteristic out-of-plane height of the magnetic field structure dl, a lower bound on the approximate magnetic field strength B, and the length of the reconnection region Δx.

Time (ns)	Δz (μm)	$\lvert\int \mathbf{B}\times\mathbf{dl}\rvert$ (MG μm)	dl (μm)	B (MG)	Δx (μm)
0.9	275±15	>160±15	∼300	$\gtrsim$0.55	1450±130
1.3	275±15	>160±15	∼500	$\gtrsim$0.30	1950±130
1.8	305±20	>180±20	∼700	$\gtrsim$0.25	2800±190

The evolution of these features, (1) the reconnection-induced electron jets and (2) the bulk magnetic fields in the interaction region, suggests that while fast reconnection occurs at early times, the mechanisms that enable this process shut off at late times. In this regime of reconnection, both strong plasma flows that force flux pileup and plasma conditions favorable to two-fluid reconnection are likely needed to produce a very fast re-

connection [24], at rates above those expected based on the initial magnetic field strength and Alfvén speed, as has been observed in previous experiments [16]. In these experiments, these criteria are achieved during the initial collision of the plasmas, but are not achieved later, coinciding with observations that are consistent with a rapid reconnection early, but minimal reconnection late.

The importance of strong plasma flows and flux pileup at early times (0.6-0.9 ns) is apparent from a comparison of relevant pressure sources, as inferred from simulated and measured quantities. 2D DRACO radiation-hydrodynamics simulations [36] were performed of colliding plasmas with an identical laser drive to that used in the experiments (albeit restricted to 2D azimuthal symmetry – with a hemispherical plasma bubble effectively interacting with a surrounding plasma torus). Laser-foil experiments on OMEGA at a similar laser intensity have validated DRACO thermal transport models [39], and so DRACO-simulated density, temperature, and flow velocity are used here [40]. The DRACO simulations show at early times an electron density of $n_e{\sim}10^{20}$ cm^{-3} (ion density $n_i = n_e/Z$, for fully ionized CH with average $Z = 3.5$), electron temperature of $T_e{\sim}1.3$ keV, ion temperature of $T_i{\sim}0.8$ keV, and flow velocity of $V{\sim}700$ μm/ns at the perimeter of the expanding plasmas just prior to their collision. The DRACO-simulated flow velocity is consistent with the experimentally estimated ∼500-1000 μm/ns expansion speed of the plasma bubbles in the proton radiography data and the time between laser onset and the collision of the plasmas. The proton radiography data give a lower-bound magnetic field strength of B $\gtrsim$0.55 MG (consistent with magnetic field measurements from previous similar experiments [14, 16]). Based on these quantities, the ratio β of thermal pressure ($n_e k T_e + n_i k T_i$) to magnetic pressure ($B^2/2\mu_0$) was $\lesssim$20 and the ratio β_{ram} of ram pressure ($\frac{1}{2} n_i A m_p V^2$) to magnetic pressure was $\lesssim$60, indicating that plasma flows dictate the strongly-driven magnetic advection and reconnection process [16] and that magnetic flux pileup is expected to be important [24]. As the magnetic field strength is unlikely to exceed the lower-bound estimate by more than a factor of 2, β and β_{ram} are likely no more than a factor of 4 lower than the upper-bound estimate, and the plasma is well into the high-β and strongly-driven regimes.

At later times, the inflows weaken due to the plasma collision and the ram pressure likely becomes insufficient to sustain the flux compression that occurs when $\beta_{ram} \gg 1$ and $\beta_{ram} > \beta$. Notably, the ratio of β_{ram}/β is insensitive to uncertainties in the magnetic field strength. While at early times $\beta_{ram}/\beta{\sim}3$ (and $\beta \lesssim 20$), by 1.3 ns, the DRACO-predicted reduction in flow velocity to ∼350 μm/ns (and the evolution of temperature and magnetic field strength) causes that ratio to drop to $\beta_{ram}/\beta{\sim}0.9$ (while $\beta \lesssim 240$), and a further reduction in flow velocity to ∼200 μm/ns by 1.8 ns produces a ratio of $\beta_{ram}/\beta{\sim}0.4$ ($\beta \lesssim 330$). Continued flux compression is neccessary to maintain a very fast reconnection at rates greater than expected based on the uncompressed magnetic field strength. As a consequence of the slowing of the plasma flows that initially drove reconnection, the magnetic field strength and Alfvén speed are not strong enough at late times to reconnect the majority of the magnetic flux. This effect, as well as a slowing of the dissipation mechanism, plausibly contributes to the apparent inhibition of reconnection.

The inferred weakening of the reconnection process may also be attributed to an evolution of plasma conditions from collisionless to collisional (from a fast, two-fluid regime to a slow, single-fluid regime of reconnection).

Two-fluid reconnection effects were likely significant early in the reconnection process, around 0.6-0.9 ns, but weaker at later times. Based on the plasma conditions stated above at 0.6-0.9 ns, the ion inertial length was $d_i = c/\omega_{pi}{\sim}30$ μm, and similarly, the ion gyroradius, the length over which ions are tied to magnetic field lines, was ρ_i ∼40 μm. On scales shorter than d_i or ρ_i, the ions are unmagnetized and the magnetic field is frozen into the electron fluid. The width of the reconnection region based on Sweet-Parker (single-fluid) reconnection theory [7, 8] was approximately $\delta_{SP} = L/\sqrt{S}$ ∼25 μm, based on the proton-radiography-measured current sheet length $L{\sim}1$ mm and a Lundquist number of $S \gtrsim 1800$. Consequently, as the ratios $\delta_{SP}/d_i \lesssim 0.8$ and $\delta_{SP}/\rho_i \gtrsim 0.6$ were less than unity, the ions were decoupled from the electrons over the reconnection region and two-fluid effects were likely important during the initial collision of the plasmas. By 1.3 ns, the plasma conditions became significantly more collisional ($T_e{\sim}1.1$ keV, $n_e{\sim}4{\times}10^{20}$ cm^{-3}, $B \gtrsim 0.3$ MG, $L{\sim}2.3$ mm, $S \gtrsim 900$, $\rho_i \lesssim 70$ μm, $d_i{\sim}16$ μm) and by 1.8 ns the plasma was well into the single-fluid regime ($T_e{\sim}0.7$ keV, $n_e{\sim}6{\times}10^{20}$ cm^{-3}, $B \gtrsim 0.25$ MG, $L{\sim}3.1$ mm, $S \gtrsim 400$, $\rho_i \lesssim 70$ μm, $d_i{\sim}13$ μm): δ_{SP}/d_i increased from $\lesssim$0.8 at 0.9 ns to $\lesssim$5.0 at 1.3 ns to $\lesssim$12 at 1.8 ns; δ_{SP}/ρ_i increased from $\gtrsim$0.6 at 0.9 ns to$\gtrsim$1.1 at 1.3 ns to $\gtrsim$2.3 at 1.8 ns.

The evolution of the DRACO-simulated electron density and electron temperature, and approximate bounds on the Lundquist number (lower bound) and the ratio δ_{SP}/d_i (upper bound) based on those parameters and the proton-radiography-estimated lower-bound magnetic field strength is depicted in Figure 3. Though these quantities should be taken as an approximate description of the plasma conditions, based on bounds and ignoring potential flux pileup effects, the trends illustrate a clear increase in collisionality. As the plasma becomes collisional, around $\delta_{SP}/d_i > 1$, two-fluid mechanisms that enable a fast reconnection diminish. It has been observed previously in tenuous plasma experiments that the reconnection rate slows significantly as the reconnection current sheet transitions from collisionless to collisional regimes [10]; the present data provide the first possible evidence of this process in a high-β, strongly-driven

plasma.

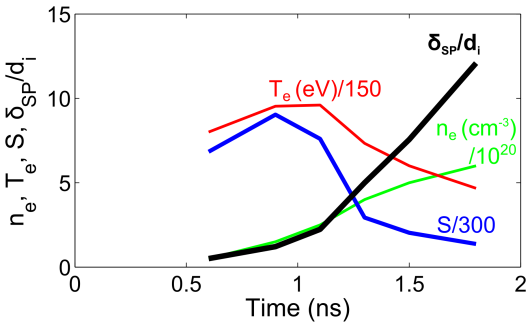

FIG. 3. (Color online) DRACO-simulated electron density (n_e, green) and electron temperature (T_e, red) around the collision region as a function of time. As the density increases and the temperature decreases, the Lundquist number lower bound (S, blue) decreases and the collisionality upper bound (δ_{SP}/d_i, thick black) increases and the plasma enters the regime of single-fluid reconnection.

In summary, data showing the evolution of magnetic reconnection behavior from fast jets to the establishment of a stable current sheet, in concert with simulated results, demonstrate that both the strength of plasma fluid flows and collisionality can potentially be important physical properties dictating reconnection dynamics even in plasmas where reconnection is strongly externally driven, and that a powerful initial drive is not sufficient to achieve a complete reconnection of magnetic fields. A combination of DRACO simulations and experimental data show that a transition between collisionless and collisional plasma conditions occurs alongside a weakening of the strong inflows that force reconnection, with both factors plausibly contributing to the observed slowing of the reconnection process. These findings are relevant to strongly-driven, high-β, two-fluid reconnection in astrophysical environments such as the magnetopause, as well as to reconnection more generally across a range of collisionality regimes. Furthermore, they motivate future experiments to resolve definitively the cause of this slowing and to address the critical question of how collisionality impacts the reconnection rate in a strongly-driven system. Future experiments may probe different regimes of strongly or weakly driven reconnection by varying laser parameters such as the peak power or the duration of the laser drive.

The authors thank the OMEGA-EP operations and target fabrication crews for their assistance with these experiments. The authors also thank Igor Igumenshchev for performing and postprocessing DRACO simulations used in this work, as well as for providing input on this manuscript. This work was performed in partial fulfillment of the first author's PhD thesis and supported in part by US DoE (Grant No. DE-NA0001857), LLE (No. 415935-G), NLUF (No. DE-NA0002035), and FSC (No. 5-24431).

* mrosenbe@mit.edu; Current institution: Laboratory for Laser Energetics, University of Rochester

[1] D. Biskamp, *Magnetic Reconnection in Plasmas* (Cambridge University Press, Cambridge, UK, 2000).
[2] B. U. O. Sonnerup, G. Paschmann, I. Papamastorakis, N. Sckopke, G. Haerendel, S. J. Bame, J. R. Asbridge, J. T. Gosling, and C. T. Russell, J. Geophys. Res. **86**, 10049 (1981).
[3] S. Tsuneta, Astrophys. J. **456**, 840 (1996).
[4] J. A. Wesson, Nucl. Fusion **30**, 2545 (1990).
[5] Y. E. Litvinenko, Astrophys. J. **515**, 435 (1999).
[6] M. Opher, J. F. Drake, K. M. Schoeffler, J. D. Richardson, R. B. Decker, and G. Toth, Astrophys. J. **734** (2011).
[7] P. A. Sweet, in *Electronmagnetic Phenomena in Cosmical Physics*, edited by B. Lehnert (Cambridge University Press, New York, 1958) p. 123.
[8] E. N. Parker, J. Geophys. Res. **62**, 509 (1957).
[9] M. Oieroset, T. D. Phan, M. Fujimoto, R. P. Lin, and R. P. Lepping, Nature **412**, 414 (2001).
[10] M. Yamada, Y. Ren, H. Ji, J. Breslau, S. Gerhardt, R. Kulsrud, and A. Kuritsyn, Phys. Plasmas **13** (2006).
[11] Y. Ren, M. Yamada, H. Ji, S. P. Gerhardt, and R. Kulsrud, Phys. Rev. Lett. **101**, 85003 (2008).
[12] T. D. Phan, J. T. Gosling, G. Paschmann, C. Pasma, J. F. Drake, M. Oieroset, D. Larson, R. P. Lin, and M. S. Davis, Astrophys. J. Lett. **719**, L199 (2010).
[13] M. Desroche, F. Bagenal, P. A. Delamere, and N. Erkaev, J. Geophys. Res. **117** (2012).
[14] C. K. Li, F. H. Séguin, J. A. Frenje, J. R. Rygg, R. D. Petrasso, R. P. J. Town, O. L. Landen, J. P. Knauer, and V. A. Smalyuk, Phys. Rev. Lett. **99**, 055001 (2007).
[15] L. Willingale *et al.*, Phys. Plasmas **17**, 043104 (2010).
[16] M. Rosenberg, C. Li, W. Fox, I. Igumenshchev, F. Séguin, R. Town, J. Frenje, C. Stoeckl, V. Glebov, and R. Petrasso, Nature communications **6**, 6190 (2015).
[17] G. Fiksel, W. Fox, A. Bhattacharjee, D. H. Barnak, P.-Y. Chang, K. Germaschewski, S. X. Hu, and P. M. Nilson, Phys. Rev. Lett. **113**, 105003 (2014).
[18] P. M. Nilson *et al.*, Phys. Rev. Lett. **97**, 255001 (2006).
[19] M. J. Rosenberg, J. S. Ross, C. K. Li, R. P. J. Town, F. H. Séguin, J. A. Frenje, D. H. Froula, and R. D. Petrasso, Phys. Rev. E **86**, 056407 (2012).
[20] P. M. Nilson *et al.*, Phys. Plasmas **15**, 092701 (2008).
[21] J. Zhong *et al.*, Nature Physics **6**, 984 (2010).
[22] Q.-L. Dong *et al.*, Phys. Rev. Lett. **108**, 215001 (2012).
[23] Q.-L. Dong *et al.*, J. Plasma Physics **78**, 497 (2012).
[24] W. Fox, A. Bhattacharjee, and K. Germaschewski, Phys. Rev. Lett. **106**, 215003 (2011).
[25] L. J. Waxer *et al.*, Opt. Photonics News **16** (2005).
[26] R. D. Petrasso *et al.*, Phys. Rev. Lett. **103**, 085001 (2009).
[27] A. J. Mackinnon *et al.*, Rev. Sci. Inst. **75**, 3531 (2004).
[28] N. L. Kugland, D. D. Ryutov, C. Plechaty, J. S. Ross, and H.-S. Park, Rev. Sci. Inst. **83**, 101301 (2012).
[29] S. P. Hatchett *et al.*, Phys. Plasmas **7**, 2076 (2000).
[30] R. A. Snavely *et al.*, Phys. Rev. Lett. **85**, 2945 (2000).
[31] A. B. Zylstra *et al.*, Review of Scientific Instruments **83**,

10 (2012).
[32] D. S. Hey, M. H. Key, A. J. Mackinnon, A. G. MacPhee, P. K. Patel, R. R. Freeman, L. D. V. Woerkom, and C. M. Castaneda, Rev. Sci. Inst. **79** (2008).
[33] C. K. Li *et al.*, Phys. Rev. Lett. **99**, 015001 (2007).
[34] M. A. Shay, J. F. Drake, and M. Swisdak, Phys. Rev. Lett. **99**, 155002 (2007).
[35] T. D. Phan, J. F. Drake, M. A. Shay, F. S. Mozer, and J. P. Eastwood, Phys. Rev. Lett. **99**, 255002 (2007).
[36] D. Keller, T. J. B. Collins, J. A. Delettrez, P. W. McKenty, P. B. Radha, B. Whitney, and G. A. Moses, Bull. Am. Phys. Soc. **44** (1999).
[37] A. Bhattacharjee, Y.-M. Huang, H. Yang, and B. Rogers, Physics of Plasmas **16**, 112102 (2009).
[38] W. Fox, A. Bhattacharjee, and K. Germaschewski, Phys. Plasmas **19**, 056309 (2012).
[39] S. X. Hu, V. A. Smalyuk, V. N. Goncharov, S. Skupsky, T. C. Sangster, D. D. Meyerhofer, and D. Shvarts, Phys. Rev. Lett. **101**, 055002 (2008).
[40] A goal of future work is to use the soon-implemented Thomson scattering system to measure these properties directly on OMEGA-EP.